

Optical absorption of Co^{2+} in ZnO

P. Koidl

Institut für Angewandte Festkörperphysik der Fraunhofer-Gesellschaft, Eckerstrasse 4, D-7800 Freiburg, West Germany

(Received 28 October 1976)

Polarized-optical-absorption spectra of Co^{2+} in ZnO are reported. The crystal-field transitions from the 4A_2 ground state to the 4T_2 (F), 4T_1 (F), and 2E (G) multiplets are analyzed in detail. These bands consist of sharp zero-phonon lines and their vibronic sidebands, where coupling to 528-cm^{-1} optical phonons and 100-cm^{-1} acoustical phonons from the M point of the ZnO Brillouin zone is shown to be dominant. In order to explain the level scheme derived from the spectra the Hamiltonian describing cubic and trigonal crystal field, Coulomb and spin-orbit interaction has been diagonalized within the full d^7 configuration. With $Dq = 400$, $v = 120$, $v' = 320$, $B = 760$, $C = 3500$, and $\zeta = 430\text{ cm}^{-1}$ both the band positions and the electronic-fine-structure splittings are satisfactorily accounted for. In addition the g factors of the Co^{2+} ground state, $g_{||}$ and g_{\perp} , are correctly predicted.

I. INTRODUCTION

In this paper optical-absorption spectra of substitutional Co^{2+} ions in ZnO are presented and their fine structure is analyzed. This investigation extends our previous work^{1,2} on Co^{2+} in cubic and hexagonal ZnS to centers with a stronger trigonal distortion. Whereas in ZnS: Co^{2+} even weak Jahn-Teller interactions were found to modify the spectra considerably,¹ the axial crystal field present in ZnO stabilizes the Co^{2+} center against Jahn-Teller effects. This is one of the main results of the present work.

Spectroscopic studies of ZnO: Co^{2+} reported in the literature^{3,4} were restricted mainly to the visible absorption band. This band, however, is a poor candidate for studying the fine structure, since transitions to all 15 spin-orbit states deriving from the 4P and 2G free-ion terms overlap. In addition, electron-phonon coupling and photoionization of the Co^{2+} ions⁵ lead to additional structure and broadening of the visible spectrum.

We shall concentrate primarily on the two lowest crystal-field transitions. A careful examination of these absorption bands revealed that Co^{2+} in ZnO is one of the rare cases where the details of the spectra can be explained by static crystal-field theory. The calculations not only predict the positions of the absorption bands, but also their electronic-fine-structure splittings, as well as the g factors of the Co^{2+} ground state.

II. THEORY

The energy levels of Co^{2+} ($3d^7$) in ZnO are determined by the following Hamiltonian:

$$H_0 = H_{\text{Cb}} + H_{\text{cf}}(T_d) + H_{\text{cf}}(C_{3v}) + H_{\text{so}} \quad (1)$$

describing Coulomb, crystal field, and spin-orbit interaction. The level scheme for the lower states

(deriving from the free-ion ground state 4F) is shown in Fig. 1.⁶ In C_{3v} symmetry only Kramers doublets remain which transform as $E_{1/2}$ and $E_{3/2}$ of the C_{3v} double group.

Within the framework of crystal-field theory the magnitude of the interactions (1) is characterized by the following radial integrals: the Racah parameters B and C describing Coulomb interaction of the seven d electrons; the cubic and trigonal crystal-field parameters Dq , v , and v' ; and the one-electron spin-orbit coupling constant ζ .

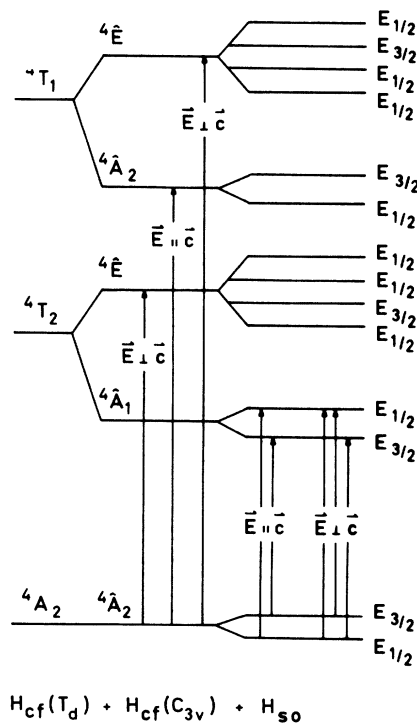


FIG. 1. Lower-energy levels of Co^{2+} in tetrahedral and trigonal symmetry (not to scale).

Macfarlane^{7,8} has calculated matrix elements of the Hamiltonian (1) between all states of the d^3 (or d^7) configuration. For a given set of the parameters B , C , Dq , v , v' , and ζ numerical diagonalization of the resulting matrices for the representations $E_{1/2}$ and $E_{3/2}$ yields the theoretical level scheme.

The gross features of the spectrum are determined by Coulomb and cubic field interaction. The corresponding parameters were fixed by fitting the eigenvalues of H_0 (assuming $v=v'=\zeta=0$) to the first moments measured for the crystal-field transitions from 4A_2 to ${}^4T_2(F)$, ${}^4T_1(F)$, ${}^4T_1(P)$, and ${}^2E(G)$. The resulting values

$$B = 760, C = 3500, Dq = 400 \text{ cm}^{-1} \quad (2)$$

are typical for Co^{2+} in tetrahedral coordination.

Using these parameters the dependence of the trigonal field splittings of the 4T states on v and v' was calculated by diagonalizing H_0 (taking $\zeta=0$). The following approximate relationships were found:

$$\begin{aligned} \text{energy } (\hat{E}) - \text{energy } (\hat{A}) \\ {}^4T_2(F): \frac{1}{2}v, \\ {}^4T_1(F): \frac{3}{4}v + 2v', \\ {}^4T_1(P): \frac{3}{4}v - 2v'. \end{aligned} \quad (3)$$

These relations are applicable in explaining the spectra if trigonal field splittings are larger than spin-orbit splittings, which is the case for most bands in $\text{ZnO}:\text{Co}^{2+}$. In addition, the ground-state splitting (Fig. 1) known from ESR⁹ to be 5.5 cm^{-1} is resolved for some transitions. Thus polarization selection rules, as indicated in Fig. 1, will permit the determination of the symmetry of the states involved in those transitions.

Besides trigonal field and spin-orbit interaction, phonon-assisted transitions contribute to the fine structure of the bands. The energy of phonons from critical points of the ZnO Brillouin zone have been determined by ir absorption,¹⁰ Raman,¹¹ electron¹² and neutron scattering experiments.¹³ A given phonon may lead to an electric-dipole-allowed sideband of the electronic transition $\Gamma_i \rightarrow \Gamma_f$ if the irreducible representation of the phonon Γ_{ph} in the defect point group (i.e., the symmetry of those normal vibrations of the Co^{2+} cluster excited by the phonon) is contained in the direct product of the representation of the initial and final electronic states and the electric dipole operator

$$\Gamma_{ph} \subset \Gamma_i \times \Gamma_{E1} \times \Gamma_f. \quad (4)$$

III. EXPERIMENTAL

ZnO crystals with dimensions of several mm^3 were grown by F. Friedrich of this laboratory

using chemical transport with chlorine acting as a transport agent. Doping with Co in concentrations ranging from 1 ppm to 1% was achieved by adding CoO to the starting material.

Optical spectra at 4.2 K were recorded with a Spex 1700 II monochromator modified for double-beam operation.¹⁴

IV. SPECTRA

The absorption spectrum of Co^{2+} in ZnO consists of three prominent bands. The long-wavelength band around $2.5 \mu\text{m}$ corresponds to the transition ${}^4A_2 \rightarrow {}^4T_2(F)$. Absorption into the ${}^4T_1(F)$ term leads to a band at $1.5 \mu\text{m}$.

Transitions into ${}^4T_1(P)$ and the terms arising from 2G lead to a broad band in the visible. All these absorption bands are polarized, the axial (α) spectra being identical with the σ spectra ($\vec{E} \perp \vec{C}$). This implies that the optical absorption of Co^{2+} in ZnO results from electric dipole transitions.

A. ${}^4T_2(F)$ band

The low-energy onset of the 4T_2 band is shown in Fig. 2. It consists of two line doublets. The smaller separation of 5.4 cm^{-1} obviously represents the ground-state splitting and confirms the value $5.5 \pm 0.3 \text{ cm}^{-1}$ determined by ESR.⁹ The two final states are separated by 19 cm^{-1} . Their symmetry has been determined from the polarization of the lines,¹⁵ as indicated in Fig. 2(b).

The remaining structure of the 4T_2 band is shown

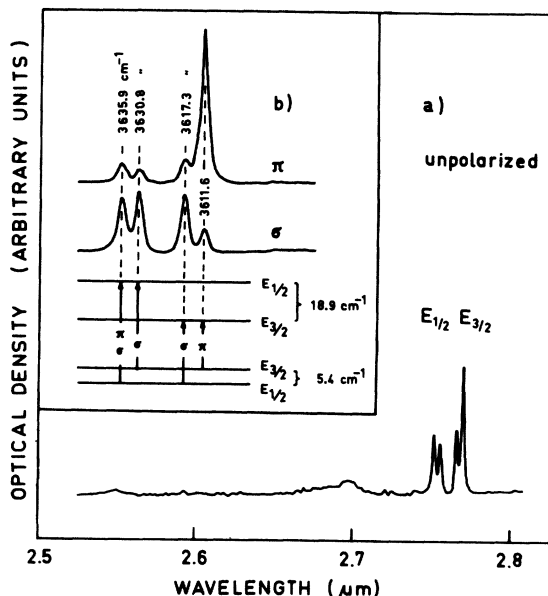


FIG. 2. Long-wavelength part of the ${}^4A_2 \rightarrow {}^4T_2(F)$ absorption of $\text{ZnO}:\text{Co}^{2+}$ (1%) taken at 4.2 K with (a) unpolarized, (b) polarized light.

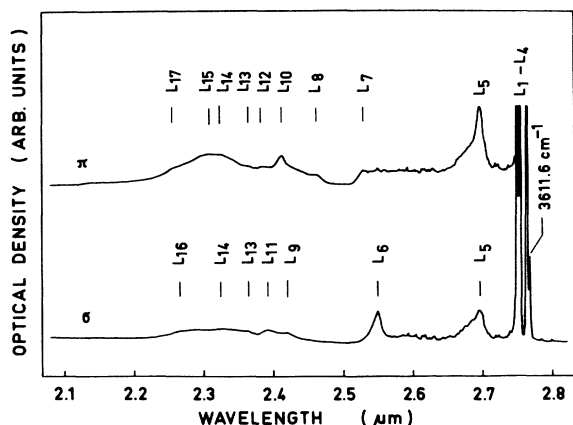


FIG. 3. ${}^4A_2 \rightarrow {}^4T_2(F)$ absorption band of $\text{ZnO}:\text{Co}^{2+}$ (1%) at 4.2 K. To avoid overlap of the spectra, the sharp lines (L_1 to L_4) are not shown for π polarization.

in Fig. 3. It is concluded that the trigonal splitting of 4T_2 cannot be greater than the spin-orbit splitting. Otherwise the selection rules for transitions between C_{3v} orbital states (Fig. 1) would govern the spectrum and σ -polarized transitions should be much more intense than the π spectrum. This is obviously not the case. From (3) we therefore get as a first information $|v| \lesssim \xi$.

The interpretation of the fine structure of the 4T_2 band is given in Table I. The assignment of lines L_1 – L_8 to the zero-phonon transitions is based on the crystal-field calculation described later.

Lines L_9 – L_{17} are interpreted as phonon-assisted transitions. Note the appearance of a 530-cm^{-1} sideband, L_{10} , which will also be prominent in the ${}^4T_1(F)$ band.

B. ${}^4T_1(F)$ band

The transition ${}^4A_2 \rightarrow {}^4T_1(F)$ leads to a strongly anisotropic band as shown in Fig. 4. The low-energy part is mainly π polarized while at higher energies σ polarization dominates. This shows, that, in contrast to the 4T_2 band, the trigonal splitting is comparable or larger than spin-orbit splittings and implies that the trigonal \hat{A}_2 component of ${}^4T_1(F)$ lies below \hat{E} .

Fig. 4 shows the occurrence of vibrational replica involving two different frequencies:

(a) Under π polarization the four strongest lines are repeated after 528 cm^{-1} . In addition, there are sidebands separated 528 cm^{-1} and twice that value from line L_{12} .

(b) At 77 K a hot band 100 cm^{-1} below L_1 is observed. This line corresponds to the lowest electronic transition starting from a thermally excited vibrational state. We therefore have to check whether lines L_2 – L_5 which also have adjacent spacings of about 100 cm^{-1} result from the emission of those phonons. This will turn out to be partly the case.

Figure 5 shows the low-energy part of the ${}^4T_1(F)$ band in more detail. For the lines L_1 – L_4 the ground-state splitting is resolved. From the po-

TABLE I. Fine structure of the ${}^4T_2(F)$ band of $\text{ZnO}:\text{Co}^{2+}$.

Line	Polarization	Energy (cm^{-1})	Difference (cm^{-1})	Assignment
L_1	π	3611.6	0	} zpl ^a $E_{3/2}$
L_2	σ	3617.3	5	
L_3	σ	3630.8	19	} zpl $E_{1/2}$
L_4	π, σ	3635.9	24	
L_5	π, σ	3711	99	zpl and/or $L_1 + TA_2$
L_6	σ	3921	309	zpl
L_7	π	3952	340	zpl
L_8	π	4057	445	zpl and/or $L_1 + \text{opt.ph.}$
L_9	σ	4129	517	} ($L_1 - L_5$) + opt.ph.
L_{10}	π	4142	530	
L_{11}	σ	4178	566	
L_{12}	π	4194	582	
L_{13}	π, σ	4227	615	} $L_5 + \text{opt.ph.}$
L_{14}	π, σ	4300	688	
L_{15}	π	4328	716	} $L_6, L_7 + \text{opt.ph.}$
L_{16}	σ	4412	800	
L_{17}	π	4429	817	

^a zpl is zero phonon line.

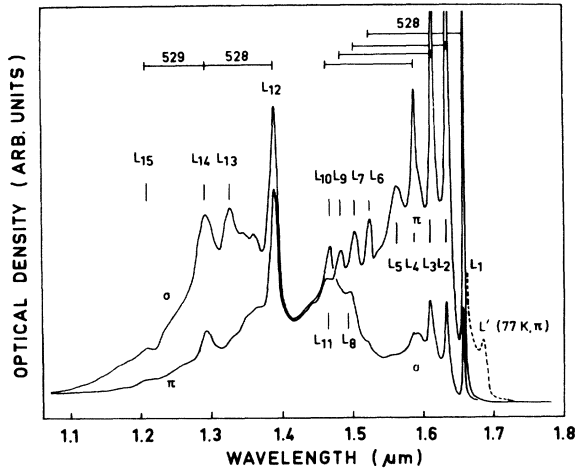


FIG. 4. ${}^4A_2 \rightarrow {}^4T_1(F)$ absorption band of ZnO:Co $^{2+}$ (1%) at 4.2 K. The dashed curve represents a hot band observed at 77 K.

larization of L_1 the symmetry of the lowest spin-orbit component of ${}^4T_1(F)$ is determined to be $E_{1/2}$. Lines L_2 are broader than L_1 and may be attributed to the emission of a phonon of 96 cm^{-1} . Lines L_3 are zero-phonon transitions to an $E_{3/2}$ state. This is concluded from the sharpness and polarization of these lines. The transitions L_4 again may be interpreted as vibrational sidebands of L_3 , the corresponding phonon having an energy of 101 cm^{-1} .

In ZnO two phonons at critical points have an energy of 101 cm^{-1} : the lowest optical mode E_2 at the

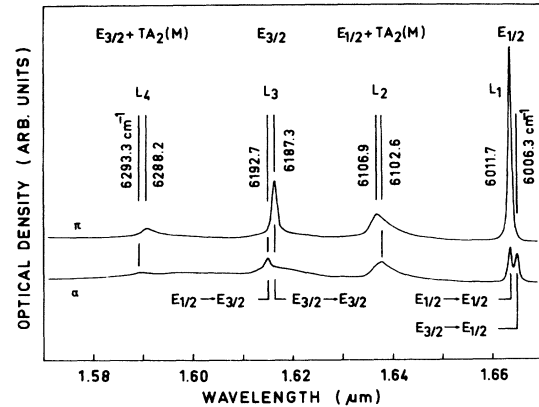


FIG. 5. Long-wavelength part of ${}^4A_2 \rightarrow {}^4T_1(F)$ absorption at 4.2 K. Axial (α) and perpendicular (π) polarized spectra were taken from different ZnO crystals containing 10 ppm (π) and 180 ppm (α) of cobalt.

Γ point¹¹ and the lowest acoustical phonon at the M point of the Brillouin zone.^{10, 12} Using space-group reduction coefficients¹⁶ it is found that the representation of the latter phonon in C_{3v} is $\hat{A}_1 + \hat{E}$ while the representation of the $E_2(\Gamma)$ mode is only \hat{E} .

The occurrence of a sideband of the electronic transition $E_{3/2} \rightarrow E_{3/2}$ under π polarization ($\Gamma_{E_1} = \hat{A}_1$) is only possible [cf. Eq. (4)], if the vibration involved has \hat{A}_1 symmetry. The polarization of the other sidebands is compatible with this statement. Thus the 100 cm^{-1} sidebands arise from zone-boundary acoustical phonons $TA_2(M)$.

TABLE II. Fine structure of the ${}^4T_1(F)$ band of ZnO:Co $^{2+}$.

Line	Polarization	Energy (cm $^{-1}$)	Difference (cm $^{-1}$)	Assignment
L' (77K)	(π)	5912	-100	$L_1 - TA_2(M)$
L_1	σ	6006.3	0	} zpl ^a $E_{1/2}$
	π, σ	6011.7		
L_2	σ	6102.6	96	} $L_1 + TA_2(M)$
	π	6106.9		
L_3	π	6187.3	181	} zpl $E_{3/2}$
	σ	6192.7		
L_4	π	6288	281	} $L_3 + TA_2(M)$
	σ	6293		
L_5	π	6387	375	$L_3 + 2TA_2(M)$
L_6	$\pi(\sigma)$	6539	527	$L_1 + \text{opt.ph.}$
L_7	π	6633	621	94 $L_2 + \text{opt.ph.}$
L_8	σ	6669	657	zpl
L_9	π	6713	701	174 $L_3 + \text{opt.ph.}$
L_{10}	σ	6793	781	zpl
L_{11}	π	6803	791	284 $L_4 + \text{opt.ph.}$
L_{12}	σ, π	7161	1149	0 zpl
L_{13}	σ	7504	1492	zpl
L_{14}	σ, π	7687	1675	528 $L_{12} + \text{opt.ph.}$
L_{15}	σ, π	8218	2206	1057 $L_{12} + 2\text{ opt.ph.}$

^azpl is zero phonon line.

We now return to the interpretation of the electronic transitions. So far it has been shown, that the lowest spin-orbit component of ${}^4T_1(F)$ is $E_{1/2}$. The next higher one has $E_{3/2}$ symmetry and lies 181 cm^{-1} above $E_{1/2}$. These states derive from the ${}^4\hat{A}_2$ component of ${}^4T_1(F)$. The remaining four spin-orbit states result from ${}^4\hat{E}$. The corresponding transitions should therefore be mainly σ polarized. If we assign the most intense lines in the σ spectrum (except L_{14} , the 528 cm^{-1} sideband of L_{12}) to these transitions, we obtain the interpretation of the ${}^4T_1(F)$ fine structure listed in Table II.

C. Visible band

The visible absorption band of $\text{ZnO}:\text{Co}^{2+}$, shown in Fig. 6, is centered at 16460 cm^{-1} and is over 3000 cm^{-1} broad. In this energy region the ${}^4T_1(P)$ term as well as the states deriving from 2G are expected. The intensity and polarization of the band, however, are determined by the spin-allowed transition to ${}^4T_1(P)$. From the anisotropy of this spectrum it follows that the trigonal splitting of ${}^4T_1(P)$ is such, that \hat{E} lies below \hat{A}_2 . This order of splitting is expected if, after (3), $2|v'| > \frac{3}{4}|v|$.

Figure 7 shows the onset of the visible band. The sharp pair of lines observed under σ polarization represents transitions from the ground-state doublet to an $E_{1/2}$ state. This is an agreement with Zeeman measurements⁴ from which it has been concluded, that the final state is $E_{1/2}$ of ${}^2E(G)$. The next pair of lines (15180.1 cm^{-1} π and 15185.9 cm^{-1} σ) results from transitions to an $E_{3/2}$ state and may be attributed to the $E_{3/2}$ spin-orbit level of ${}^2E(G)$. The analysis of the temperature dependence of the weak line at 15180.1 cm^{-1} in the π spectrum⁴ confirms, that this transition starts

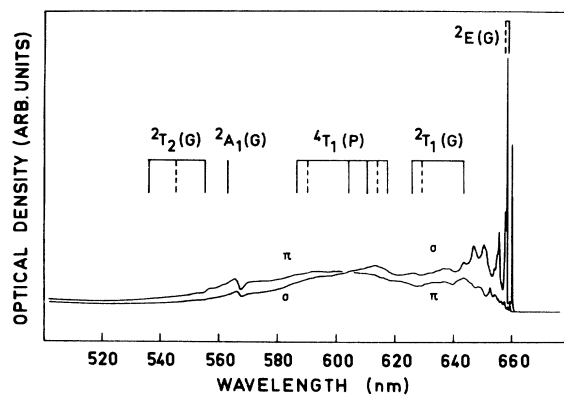


FIG. 6. Visible absorption band of $\text{ZnO}:\text{Co}^{2+}$ (10 ppm) at 4.2 K. Also indicated are the theoretical energies for $E_{1/2}$ (solid bars) and $E_{3/2}$ states (broken bars), as calculated by diagonalizing H_0 with the parameters (5), see Sec. V.

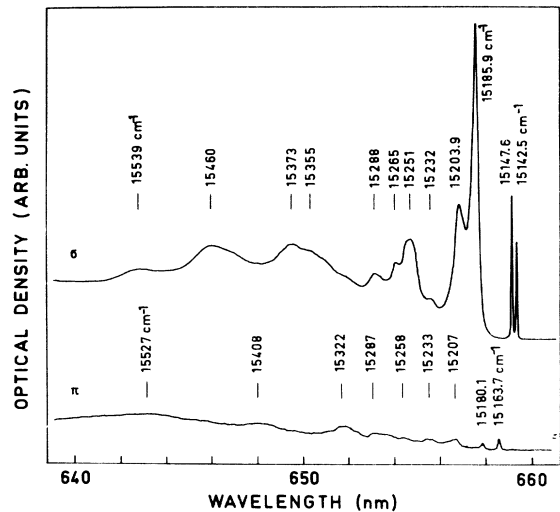


FIG. 7. Long-wavelength onset of the visible absorption band of $\text{ZnO}:\text{Co}^{2+}$ (10 ppm) at 4.2 K. The lowest line under π polarization (15163.7 cm^{-1}) results from small amounts of Ni^{2+} impurities (cf. Ref. 19).

from the thermally occupied $E_{3/2}$ (4A_2) state.

For the lines at higher energies unequivocal symmetry assignments are not possible, since the ground-state splitting is no longer resolved. We therefore shall not try to identify the remaining fine structure in detail.

However, we want to refer to the dispersionlike structure at 567 nm , superimposed on the broad vibronic ${}^4T_1(P)$ band (Fig. 6). This line can be attributed to the transition to ${}^2A_1(G)$. The antiresonant line shape of sharp transitions overlapped by a continuous vibronic band has been discussed by Sturge *et al.*¹⁷

With more heavily doped $\text{ZnO}:\text{Co}$ crystals three additional antiresonant lines are seen at 18060 , 18330 , and 18430 cm^{-1} . These energies closely correspond to those calculated for the components of ${}^2T_2(G)$ (18134 , 18338 , and 18668 cm^{-1} , see Fig. 6).

V. DISCUSSION

The level scheme of Co^{2+} in ZnO has been calculated by numerical diagonalization of the Macfarlane matrices as described in Sec. II. The parameters B , C , and Dq were fixed from the band centers, and the remaining parameters v , v' , and ζ have been varied. The best fit is obtained with the following set of parameters:

$$\begin{aligned} B &= 760, & C &= 3500, & Dq &= 400, \\ v &= 120, & v' &= 320, & \zeta &= 430 \text{ cm}^{-1}. \end{aligned} \quad (5)$$

In Table III the theoretical and observed energies

TABLE III. Energy levels of Co²⁺ in ZnO.

Term	First moment (cm ⁻¹)		Fine structure (cm ⁻¹)			
	Theoretical	Experimental	Theoretical	Experimental		
⁴ A ₂	0	0	<i>E</i> _{1/2}	0	0	<i>E</i> _{1/2}
			<i>E</i> _{3/2}	5.4	5.4	<i>E</i> _{3/2}
⁴ T ₂	4000	4070	<i>E</i> _{3/2}	0	0	<i>E</i> _{3/2}
			<i>E</i> _{1/2}	19.5	19	<i>E</i> _{1/2}
			<i>E</i> _{1/2}	112	99	
			<i>E</i> _{3/2}	291	309	
			<i>E</i> _{1/2}	341	340	
			<i>E</i> _{1/2}	420	445	
⁴ T _{1(F)}	6924	6800	<i>E</i> _{1/2}	0	0	<i>E</i> _{1/2}
			<i>E</i> _{3/2}	189	181	<i>E</i> _{3/2}
			<i>E</i> _{1/2}	673	657	
			<i>E</i> _{1/2}	988	781	
			<i>E</i> _{3/2}	1164	1149	
			<i>E</i> _{1/2}	1304	1492	
² E(<i>G</i>)	15 162	15 180	<i>E</i> _{1/2}	0	0	<i>E</i> _{1/2}
			<i>E</i> _{3/2}	21	38	<i>E</i> _{3/2}
⁴ T _{1(P)}	16 475	16 460				

are compared. It is seen that static crystal-field theory not only explains the centers of the bands, but also accounts remarkably well for their fine structure. Especially the lower spin-orbit components of the bands are correctly predicted. This interesting result is rather surprising, since in cubic and hexagonal ZnS:Co²⁺ even weak coupling to asymmetric vibrations drastically alters the static spin-orbit splittings (dynamic Jahn-Teller effect).¹ In the present case electron-phonon coupling only leads to the occurrence of vibrational sidebands.

The different behavior of Co²⁺ in ZnS and ZnO has to be attributed to the relatively strong trigonal crystal-field component present in ZnO. The axial field splitting of ⁴T_{2(F)} and ⁴T_{1(F)} is such that the orbital singlet is lowest. Within a ⁴A₁ or ⁴A₂ term, however, only vibronic coupling with totally symmetric vibrations takes place. Within a ⁴E term in C_{3v} symmetry Jahn-Teller interactions are possible. Those effects probably will cause the minor deviations between calculated and observed energies of the higher ⁴T_{1(F)} spin-orbit states.

In order to check the consistency of the parameters (5) we have calculated the *g* factor of the Co²⁺ ground state. This was achieved by numerical diagonalization of the crystal-field Hamiltonian (1), *H*₀, including the Zeeman interaction

$$H_1 = \mu_B (k\vec{L} + g_s\vec{S}) \cdot \vec{H} \quad (6)$$

within the full *d*⁷ configuration. Here μ_B is the Bohr magneton, *k* the orbital reduction factor, and $g_s = 2.0023$ the free-spin *g* factor. Matrix elements of *H*₁ have been given by Macfarlane.⁸

Using the parameters (5) we obtain

$$\begin{aligned} g_{||} &= 0.2522k + 0.99388g_s, \\ g_{\perp} &= 0.28842k + 0.99456g_s. \end{aligned} \quad (7)$$

The covalent reduction factor *k* is expected to be not much smaller than unity. Making the point-ion approximation,¹⁸ *k* = 1, we get

$$g_{||} = 2.2422, \quad g_{\perp} = 2.2798$$

which is in excellent agreement with the observed *g* values⁹:

$$g_{||} = 2.243, \quad g_{\perp} = 2.2791.$$

ACKNOWLEDGMENTS

I am indebted to F. Friedrich for growing the crystals and to A. Rauber for advice concerning the crystal growth. Furthermore I want to thank R. M. Macfarlane for making available a copy of Ref. 8.

- ¹P. Koidl, O. F. Schirmer, and U. Kaufmann, *Phys. Rev. B* **8**, 4926 (1973).
- ²P. Koidl and A. R auber, *J. Phys. Chem. Solids* **35**, 1061 (1974).
- ³H. A. Weakliem, *J. Chem. Phys.* **36**, 2117 (1962).
- ⁴R. S. Anderson, *Phys. Rev.* **164**, 398 (1967).
- ⁵Y. Kanai, *J. Phys. Soc. Jpn.* **24**, 956 (1968).
- ⁶We use Mulliken's notation for the irreducible representations of the orbital states. Those in C_{3v} are marked with a caret.
- ⁷R. M. Macfarlane, *Phys. Rev. B* **1**, 989 (1970).
- ⁸R. M. Macfarlane, IBM Research Report No. RJ 1090 (1972) (unpublished).
- ⁹T. L. Estle and M. de Wit, *Bull. Am. Phys. Soc.* **6**, 445 (1961).
- ¹⁰S. S. Mitra and R. Marshall, in *Proceeding of the Seventh International Conference on the Physics of Semiconductors, Paris, 1964* (Academic, New York, 1964).
- ¹¹C. A. Arguello, D. L. Rousseau, and S. P. S. Porto, *Phys. Rev.* **181**, 1351 (1969).
- ¹²A. W. Hewat, *Solid State Commun.* **8**, 187 (1970).
- ¹³K. Thoma, B. Dorner, G. Duesing, and W. Wegener, *Solid State Commun.* **15**, 1111 (1974).
- ¹⁴K. Leutwein, *Appl. Opt.* **10**, 46 (1971).
- ¹⁵The fact that the polarization selection rules [Fig. 2(b)] are fulfilled predominantly but not rigorously is caused most probably by mixing of the excited $E_{1/2}$ and $E_{3/2}$ states by internal strains. This is supported by the analysis of the ${}^4T_1(F)$ band. There the separation of the excited states is much larger (181 cm^{-1}) than the energies of internal strains. Consequently the polarization selection rules are strictly obeyed.
- ¹⁶U. Kaufmann and O. F. Schirmer, *Opt. Commun.* **4**, 234 (1971).
- ¹⁷M. D. Sturge, H. J. Guggenheim, and M. H. L. Pryce, *Phys. Rev. B* **2**, 2459 (1970).
- ¹⁸A more realistic assumption, $k = (\zeta/\zeta_{\text{free ion}})^{1/2} = 0.9$, yields g values smaller by about 1%.
- ¹⁹U. Kaufmann and P. Koidl, *J. Phys. C* **7**, 791 (1974).